

# Changes in ISO 6336:2019 — Parts 1, 2, 3, 5 and 6

Hanspeter Dinner

## Introduction

ISO 6336 is the most widely used and technically advanced document for cylindrical gear strength rating. It falls under the responsibility of ISO technical committee TC 60, subcommittee 2, work group WG 6 “Gear Calculations”. Convenor of WG6 is Prof. Dr. Ing. Karsten Stahl of the FZG Munich, Germany.

The third edition of ISO 6336 has been extended and now includes the now replaced ISO/TR 13989-1 and -2 on scuffing, the now replaced ISO/TR 15144-1 and -2 on micropitting, and a new part 4 on tooth flank fracture. Calculation examples form parts 30 and 31. The different parts and classification as standard, technical specification or technical report are listed in the below table.

In ISO/TR 6336-30:2017, (Ref.11), calculation examples based on ISO 6336-1:2006, (Ref. 1), ISO 6336-2:2006, (Ref. 3), ISO 6336-3:2006, (Ref. 5), ISO 6336-5:2003, (Ref. 7), are given. These documents are already replaced by the currently valid editions, but as of today, ISO/TR 6336-30:2017 is based on the prior edition. This technical report (TR) is currently being updated to represent the changes in ISO 6336-1:2019, (Ref. 1), ISO 6336-2:2019, (Ref. 4), ISO 6336-3:2019, (Ref. 6) and ISO 6336-5:2016, (Ref. 10).

The purpose of this paper is to point the reader to changes in the third edition of parts 1, 2, 3, 5 and 6 compared to the previous edition (from the year 2006 for parts 1, 2, 3, 6 and from the year 2003 for part 5). The paper is limited to a description of the changes and does not comment on their merit or their consequences. Some comments on the limitations of this paper are due:

- In the 2006 edition, a new section often started with some introductory text. In the 2019 edition, this text is put into a subsection “General” so that no body of text is directly beneath a top-level section title. This change is not mentioned

**Table 1 Parts of the ISO 6336 series**

Calculation of load capacity of spur and helical gears	International Standard	Technical Specification	Technical Report
Part 1: Basic principles, introduction and general influence factors	X		
Part 2: Calculation of surface durability (pitting)	X		
Part 3: Calculation of tooth bending strength	X		
Part 4: Calculation of tooth flank fracture load capacity		X	
Part 5: Strength and quality of materials	X		
Part 6: Calculation of service life under variable load	X		
Part 20: Calculation of scuffing load capacity — Flash temperature method		X	
Part 21: Calculation of scuffing load capacity — Integral temperature method		X	
Part 22: Calculation of micropitting load capacity		X	
Part 30: Calculation examples for the application of ISO 6336 parts 1, 2, 3, 5			X
Part 31: Calculation examples of micropitting load capacity			X

for each section.

- Only normative annexes are addressed here. Informative annexes are not documented in this paper.
- In the 2019 edition, some errors in the 2006 edition were corrected (e.g., formula for basic rack factor CB, changed from «...1.25 -  $h_{fp}$ ...» to «...1.20 -  $h_{fp}$ ...»), but such corrections are not documented.
- New parts of ISO 6336, e.g., part 4, are not documented here. They deserve a more detailed introduction outside the scope of this paper.
- Additional comments on the formulas and calculation examples for ring gears can be found in (Ref. 17).
- In all parts, a table with the abbreviated terms and symbols used in the part, is added to section 3 “Terms, definitions, symbols and abbreviated terms.”
- Bibliography has changed in all parts.

## Part 1 of ISO 6336:2019

### Overview

The scope of ISO 6336-1:2019, (Ref. 2) is defined as follows:

“This document presents the basic principles of, an introduction to, and the general influence factors for the calculation of the load capacity of spur and helical gears. Together with the other documents in the ISO 6336 series, it provides a method by which different gear designs can be compared. It is not intended to assure the performance of assembled drive gear systems. It is not intended for

use by the general engineering public. Instead, it is intended for use by the experienced gear designer who is capable of selecting reasonable values for the factors in these formulae based on the knowledge of similar designs and the awareness of the effects of the items discussed.

The formulae in the ISO 6336 series are intended to establish a uniformly acceptable method for calculating the load capacity of cylindrical gears with straight or helical involute teeth.”

The introduction section now includes above overview of the ISO 6336 documents, Table 1, as parts 4, 20, 21, 22, 30 and 31 have been added to ISO 6336 series.

This part now includes as normative reference ISO 21771:2007, (Ref. 13), for cylindrical involute gear geometry. This standard was published in 2007 and in ISO 6336:2006, no reference to such a standard was available. ISO 6336:2019 now states that terms and definitions of ISO 21771:2007 apply, along with those from ISO 1122-1:1998 (Ref. 12). With this, the gear strength rating standards are linked to gear geometry calculation standards.

## Structure of ISO 6336-1:2019, compared to previous edition

Foreword, Introduction, Sections 1, 2 and 3 maintain their structure. The

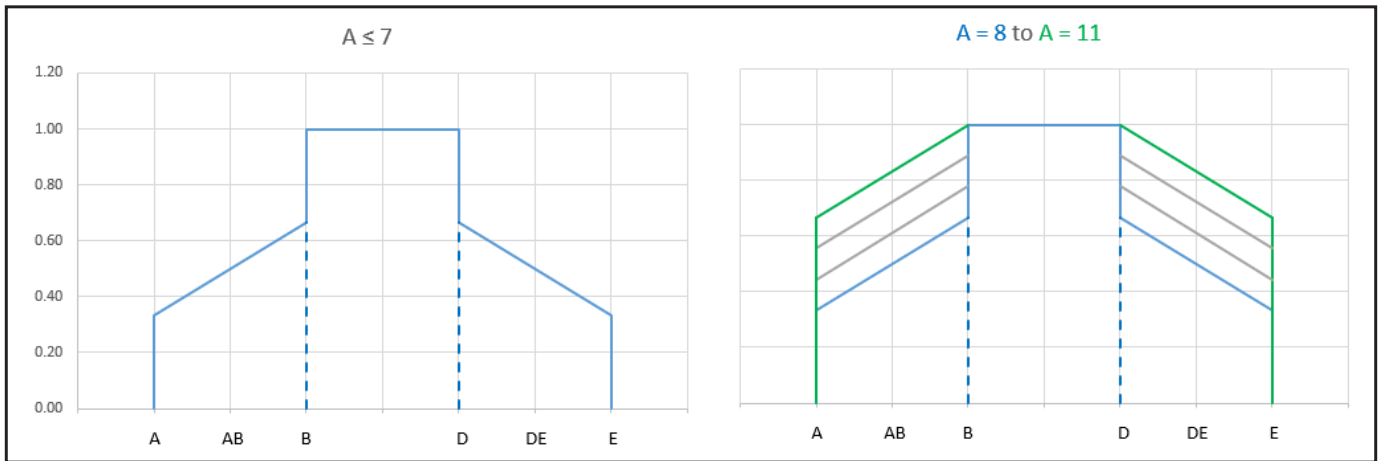


**Figure 1** Left: Load sharing factor, spur gear, unmodified profile,  $A \leq 7$ . Right: Load sharing factor, spur gear, unmodified profiles, for  $A = 8$  to  $A = 11$ .

introduction now includes an overview of all the documents belonging to ISO 6336 series, see Table 1.

Section 4, specifically section 4.1, now includes those failure modes addressed in the different parts of the standard in the same sequence as they are covered in the different part numbers. These are “Surface durability (pitting),” “Tooth bending strength,” “Tooth flank fracture,” “Scuffing” and “Micropitting.” Wear and plastic yielding are still mentioned as possible failure modes but are not covered in ISO 6336. Comments on specific areas of gearing, e.g., “Vehicle final drive gears,” “Main drive for aircraft and space vehicles” or “Industrial high-speed gears” remain included.

The section on safety factors remains as well; it is now more detailed and explains differences between different safety factors, e.g., that the safety factor for bending is calculated from two stresses while e.g., the safety factor for scuffing is calculated from two temperature levels. Both 2006 and 2019 version include the most important statement that “... Recommendations concerning these minimum values (for safety factors) are made... but values are not proposed...”

Section 5 on application factor  $K_A$  retains its structure but a subsection with guide values for the application factor, method B is added, see Table 3 below. In section 6 on the dynamic factor  $K_v$ , a section on  $K_v$  for low loaded gears,  $(F_t \times K_A \times K_y) / b < 100 \text{ N/mm}$ , has been added. Otherwise, the structure of the section is the same as in 2006 edition.

The structure of section 7 on the face

load factor  $K_{H\beta}$ , section 8 for the transverse load factors  $K_{H\alpha}$  and  $K_{F\alpha}$ , section 9 for the tooth stiffness parameters,  $c'$  and  $c_y$  and Annex A (normative), additional methods for determination of  $f_{sh}$  and  $f_{ma}$ , is the same as in 2006 edition.

A whole new section 10, Parameter of Hertzian contact, has been added in 2019 edition of ISO 6336. It originates from ISO/TR 15144-1:2014 (there, as section 10) and ISO/TR 13989-1:2000 (there, as section 9). In section 10.1, the formulas on how to calculate the normal and transverse radius of relative curvature in the contact point CP,  $\rho_{red,CP}$  and  $\rho_{red,t,CP}$  and from the transverse radius of curvature of the pinion and wheel are given (division of the product of the radii of curvature of pinion and wheel by sum of the radii of curvature of pinion and wheel). Note that the radii here are for the unmodified involute shape, not considering modifications like tip relief or similar. In a similar manner, the reduced modulus of elasticity  $E_r$  is calculated from the modulus of elasticity of the pinion and the wheel as well as from the Poisson’s ratio of pinion and wheel.

The local Hertzian contact stress  $p_{dyn,CP}$  calculated as method A through a loaded tooth contact analysis LTCA, typically using a 3D load distribution program, is defined as the local nominal Hertzian contact stress  $p_{H,CP,A}$  multiplied by the square root of  $K_A$ ,  $K_y$  and  $K_v$  (comments on these can be found above and below). For method B, no loaded tooth contact analysis is used, the load distribution is considered as additional factors (again the square root thereof)  $K_{H\alpha}$  (transverse load factor) and  $K_{H\beta}$  (face load factor).

The formula for the local contact stress in the contact point CP as per method B,  $p_{H,CP,B}$  then uses the relative radius of curvature (above), the reduced modulus of elasticity (above), the transverse tangential load at the reference cylinder  $F_t$ , the face width  $b$ , and the load sharing factor  $X_{CP}$  and is:

$$p_{H,CP,B} = \sqrt{\frac{E_r}{2 \times \pi}} \times \sqrt{\frac{F_t \times X_{CP}}{b \times \rho_{red,CP} \times \cos(\alpha_t)}}$$

In section 10.4, another very helpful formula to calculate the half of the Hertzian contact width,  $b_H$  is given as follows:

$$b_{H,CP} = 4 \times \rho_{red,CP} \times \frac{\rho_{dyn,CP}}{E_r}$$

Section 10.5 deals with the load sharing factor  $X_{CP}$  and is complex. The factor accounts for the load sharing between succeeding pairs of meshing teeth. It is defined along the path of contact, using parameter  $g_{CP}$  to describe the position of the contact. The value of  $X_{CP}$  does not exceed 1.00, where 1.00 means full transverse single tooth contact. The load sharing factor depends on the profile modifications and—for helical gears—is combined with the buttressing factor  $X_{but,CP}$ . The buttressing factor accounts for a stress increase at the start and end of the oblique contact lines on the flank in case of unmodified helical gears. Its minimum value is 1.00 and reaches a maximum of 1.30.

Section 10.5 starts with a definition of points A, AB, C, D, DE and E defined as special contact points CP, all on the path of action. If the pinion (the gear in mesh with the lower number of teeth) is driving, then, point A is the start of mesh. If the gear is driving, start of mesh is point E. It also defines the diameter of the

circles with center equal to pinion and gear center going through the contact point,  $d_{CP1}$  and  $d_{CP2}$ , both as a function of the parameter  $g_{CP}$  describing the position of the contact point CP on the path of action.

In section 10.5.2, the load sharing factor is given along the path of action (from points A to E) for spur gears with unmodified profiles, spur gears with profile modifications, helical gears with  $\epsilon_\beta \leq 0.80$  and unmodified profiles, helical gears with  $\epsilon_\beta \leq 0.80$  and modified profiles, helical gears with  $\epsilon_\beta \geq 1.20$  and unmodified profiles, helical gears with  $\epsilon_\beta \geq 1.20$  and modified profiles and helical gears with  $0.8 < \epsilon_\beta < 1.20$ . Only in case of a spur gear with unmodified profile, the load sharing factor is given for different quality classes A=8 to A=11.

Section 10.6 gives formulas on how to calculate the tangential velocities of the contact point CP on the flank of the pinion and the wheel. The two speed vectors in the contact point have the same direction (normal to the path of contact or tangential to both flanks), the velocity of the resulting speed vector is hence

equal to the sum of the velocities of the two vectors.

Section 11, Lubricant parameters at given temperature, has been added in edition 2019 of ISO 6336-1. It is the same content as in ISO/TR 15144-1:2010 (or its second edition of 2014, both withdrawn and replaced by ISO/TS 6336-22), section 7.2. Note that the identical text can again be found in ISO/TS 6336-22:2018 on micropitting. In this new section, the procedure to calculate the dynamic viscosity at a given temperature from the kinematic viscosity is given. Also, the calculation formulae for calculation of the kinematic viscosity at a given temperature from the kinematic viscosity at 40°C and 100°C are given. Finally, the formula for the calculation of the lubricant density at a given temperature from the lubricant temperature at 15°C is given in this section.

**Application**

The method for calculating the load capacity of cylindrical gears are in good agreement or validated for the below boundary conditions. Note the slight

changes between 2006 and 2019 edition for pressure and helix angle Table 2:

**Changes in formulas and factors**  
**Mesh load factor  $K_y$**

Edition 2019 now specifically includes the mesh load factor  $K_y$  in the formulas where it is—like e.g., the application factor  $K_A$ —multiplied with the nominal tangential load. This is clearer than in edition 2006 where a statement was given that  $K_A$  needs to be replaced by  $K_A \times K_y$  if a gear drives two or more mating gears. Some additional comments concerning the use of  $K_y$  are given.

Note that  $K_y$  is also used in the other parts of ISO 6336 in the formulas where in previous edition, only  $K_A$  was present. This change is not further mentioned in below sections.

**Application factor  $K_A$**

The system for describing application factors has been extended. In 2006 edition, the application factor  $K_A$  could be derived along method A or method B, becoming  $K_{A-A}$  and  $K_{A-B}$  respectively. In 2019 edition, separate application factors  $K_{HA}$  for pitting,  $K_{FA}$  for root breakage,  $K_{FFA}$  for tooth flank fracture,  $K_{\theta A}$  for scuffing,  $K_{\lambda A}$  for micropitting are introduced. Again, they can be determined along method A or B and the respective suffix is added.  $K_{FFA-B}$  for example means application factor along method B, for flank fracture calculation.

“Table 4—Application factor,  $K_A$ ” with guide values for  $K_{A-B}$  is added. Additional tables 6 and 7, with application examples, to be used in conjunction with this table, explaining the meaning of e.g., “Light shocks,” are also added in 2019 edition. With this, a practical tool to select a suitable value for  $K_{A-B}$  is available now:

**Dynamic factor  $K_v$**

In 2006 edition, a value for  $K_v > 2.00$  was possible. This means that gear flanks could separate and in 2019 edition, the dynamic factor  $K_v$ , for gears operating outside their resonance condition, shall be set  $K_{v-B}$  or  $K_{v-C} = 2.00$  if its calculated value is higher than 2.00.

The dynamic factor in the subcritical range ( $N \leq N_s$ ) and for main resonance range ( $N_s < N \leq 1.15$ ) is calculated using a parameter  $B_k$ .  $B_k$  was calculated in 2006 edition considering the tip relief  $C_a$  only.

**Table 2 Range of validity and limitations**

Property	2006 edition, limits	2019 edition, limits
Gear type	Cylindrical, external, internal	Cylindrical, external, internal
Profile geometry	Involute	Involute
Normal working pressure angle	Up to 25°	15° to 25°
Reference helix angle	Up to 25°	Up to 30°
Transverse contact ratio	1.00 to 2.50	1.00 to 2.50
Gears with $\epsilon_\alpha < 1.00$	Formulas not applicable	Formulas not applicable
ooth tips and root fillets interfere	Formulas not applicable	Formulas not applicable
Teeth are pointed	Formulas not applicable	Formulas not applicable
Backlash is zero	Formulas not applicable	Formulas not applicable

**Table 3 Guide values for application factor,  $K_{A-B}$ , as added in 2019 edition.**

Working characteristic of driving machine	Working characteristic of driven machine			
	Uniform	Light shocks	Moderate shocks	Heavy shocks
Uniform	1.00	1.25	1.50	1.75
Light shocks	1.10	1.35	1.60	1.85
Moderate shocks	1.25	1.50	1.75	2.00
Heavy shocks	1.50	1.75	2.00	≥2.25

**Table 4 Range of validity and limitations**

Property	2006 edition, limits	2019 edition, limits
Lubrication	Oil primarily, grease approximatively	Cylindrical, external, internal
Profile geometry	Basic rack as standardized in ISO 53, [15]	Basic rack as standardized in ISO 53, [15]
	Other basic racks where actual transverse contact ratio is less than $\epsilon_{\alpha n} = 2.50$	Other basic racks where actual transverse contact ratio is less than $\epsilon_{\alpha n} = 2.50$

**Table 5 Factor  $f_{Cza}$**

Condition	Value for $f_{Cza}$
Helical gear sets with suitable profile and longitudinal modifications based on the 3D load distribution program, and with the maximum contact stress near mid-height and essentially uniform stress distribution	1.00
Helical gear sets with suitable flank modifications acc. to manufacturers experience	1.07
Helical gear sets without flank modifications	1.20

In 2019 edition,  $B_k$  is calculated using  $\min(C_{a1}+C_{f2}, C_{a2}+C_{f1})$ , considering also root relief and being clear that the minimum value per gear shall be used.

Equations (25) and (26), for the calculation of the moment of inertia of a stationary and rotating ring gear in planetary gearboxes have changed. The correct index for the ring gear is now used and second instead of fourth power of the ring gear diameter is used in the denominator.

Edition 2019 of ISO 6336 references to ISO 1328-1:2013 (where lowest quality is grade 11), while edition 2006 references to ISO 1328-1:1995 (where lowest quality grade is 12). Quality grade 12 is no longer used for  $K_v$  calculation (see section 6.6.2 in ISO 6336-1:2019), lowest quality grade used is now 11.

### Face load factors $K_{H\beta}$ and $K_{F\beta}$

For calculation of  $K_{H\beta-C}$ , in case that favorable position of contact pattern is verified, the tolerance on helix slope deviation for ISO tolerance class 5 (along ISO 1328-1:2013),  $f_{H\beta 5}$  is used in edition 2019 instead of tolerance class 6 (along ISO 1328-1:1995),  $f_{H\beta 6}$  in edition 2006.

### Tooth stiffness parameters, $c'$ and $c_y$

In section 9.3.2.6, clarification is added that  $c_{y\beta}$  and  $c_{y\alpha}$  are defined in the transverse direction in the plane of action. This clarification was missing in 2006 edition.

## Part 2 of ISO 6336:2019

### Overview

The scope of ISO 6336-2:2019, (Ref. 4), is defined as follows:

“This document specifies the fundamental formulae for use in the determination of the surface load capacity of cylindrical gears with involute external or internal teeth. It includes formulae for all influences on surface durability for which quantitative assessments can be made. It applies primarily to oil lubricated transmissions, but can also be used to obtain approximate values for (slow running) grease lubricated transmissions, as long as sufficient lubricant is present in the mesh at all times.

The given formulae are valid for cylindrical gears with tooth profiles in accordance with the basic rack standardized in ISO 53. They can also be used for teeth conjugate to other basic racks where the

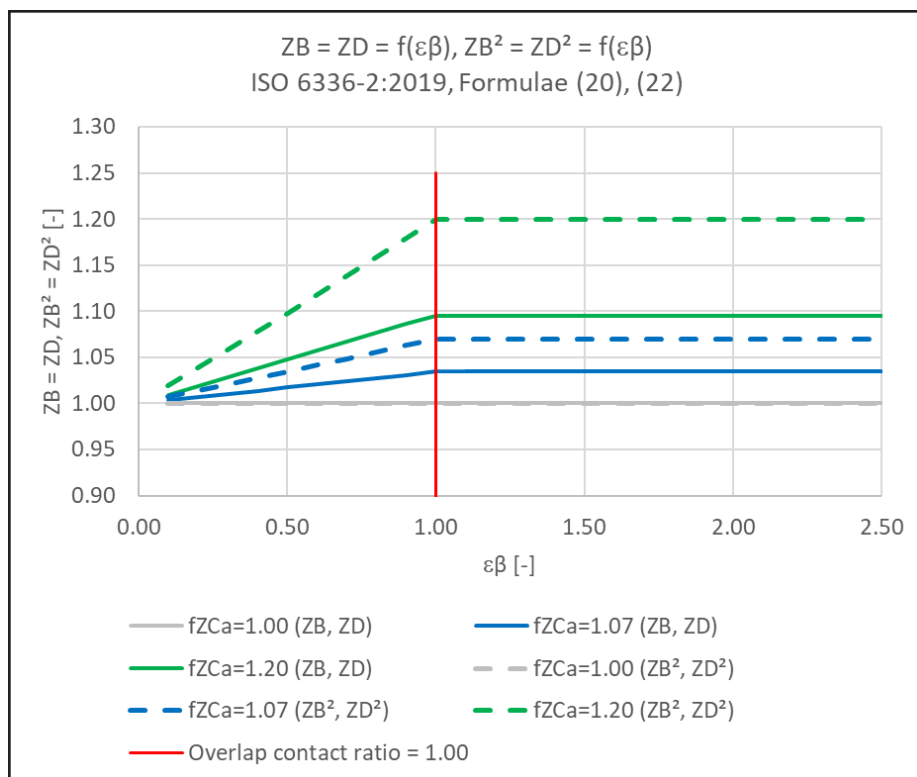


Figure 2 Zone factors  $Z_{K_{H\beta-C}} B$  and  $Z_D$  and their square as a function of  $f_{ZCa}$  and overlap contact ratio  $\epsilon_{\beta}$ .

Table 6 Material combinations considered for calculation of work hardening factor $Z_w$		
Material combinations, cases	2006 edition, material combinations considered	2006 edition, material combinations considered
Case 1	Surface-hardened pinion with through-hardened gear	Surface-hardened steel pinion with through-hardened steel gear
Case 2	Through-hardened pinion and gear	Through-hardened steel pinion with through-hardened steel gear
Case 3	NA	Surface-hardened steel pinion with ductile iron gear

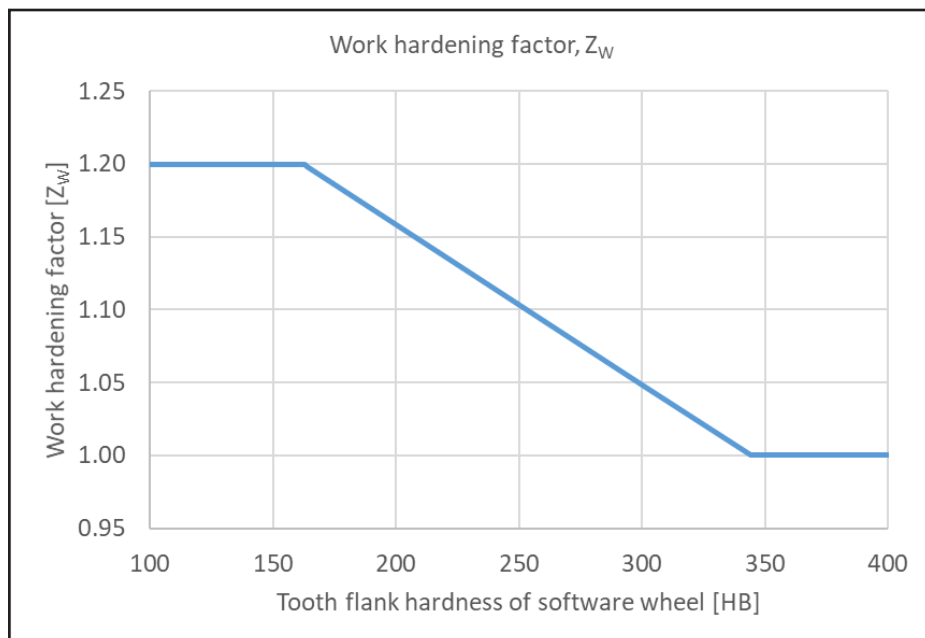


Table 7 Work hardening factor  $Z_w$ , ISO 6336-2:2019, for combination of surface-hardened steel pinion with ductile iron gear.

actual transverse contact ratio is less than  $\epsilon_{\alpha n} = 2,5$ . The results are in good agreement with other methods.”

**Structure of ISO 6336-2:2019, compared to previous edition**

The structure of the foreword, introduction and sections 1 to 12 and 14 remain the same.

In section 13, Work hardening factor,  $Z_W$ , a new subsection 13.3.3 Surface-hardened steel pinion with ductile iron gear, is added. It describes graphical values and determination by calculation of work hardening factor  $Z_W$  for the mentioned material pairing.

Annex A (informative), Start of involute, present in 2006 edition has been removed in 2019 edition.

**Application**

Further to the conditions for the application of ISO 6336 as found in part 1, see Table 2. These conditions apply, Table 4.

**Changes in formulas and factors**

Calculation of permissible contact stress for through hardened wrought steel, nitrided, nitro carburized steel

Formula (15) (it is the same formula in 2006 and in 2019 edition), for the calculation of the permissible contact stress of through hardened wrought steel, nitrided, nitro carburized, for the limited life stress range, has changed and now includes a different factor (0.7686 in 2019 edition vs. 0.7098 in 2006 edition).

**Calculation of zone factors  $Z_B$  and  $Z_D$ , diameters**

In the formulas, the active tip diameter  $d_{Na}$  is used (in edition 2019) instead of the tip diameter  $d_N$  (in 2006) edition.

**Calculation of zone factors  $Z_B$  and  $Z_D$ , auxiliary factor  $f_{ZCa}$**

For helical gears with  $\epsilon_{\alpha} > 1.00$  and  $\epsilon_{\beta} \geq 1.00$  (section 6.3, clause b) as well as for helical gears with  $\epsilon_{\alpha} > 1.00$  and  $\epsilon_{\beta} < 1.00$  (section 6.3, clause c), a new auxiliary factor  $f_{ZCa}$  is introduced and used for the calculation of the zone factors  $Z_B$  and  $Z_D$ :

For helical gears with  $\epsilon_{\alpha} > 1.00$  and  $\epsilon_{\beta} \geq 1.00$ , zone factors  $Z_B$  and  $Z_D$  are not  $Z_B = Z_D = 1.00$  anymore (as in 2006 edition) but  $Z_B = Z_D = f_{ZCa}^{0.5}$ . Contact stress is hence increased by  $f_{ZCa}^{0.5}$  or

transmittable torque is reduced by  $1/f_{ZCa}$ .

**Transverse and overlap contact ratio  $\epsilon_{\alpha}$  and  $\epsilon_{\beta}$**

Instead of root form and tip diameters (in edition 2006), active root and active tip diameters (in edition 2019) are used for determination of contact ratios.

**Lubricant factor  $Z_L$**

The table listing viscosity parameters (nominal viscosity  $\nu_{40}$ ,  $\nu_{50}$ , viscosity parameter  $\nu_j$ ) now includes the parameters for additional viscosity grades, VG10, VG15 and VG22. These values are used for determination of the lubricant factor  $Z_L$  by calculation.

**Factor  $Z_W$**

In 2006 edition, two cases were considered for the gears in mesh material combinations whereas in 2019, a third case has been added as listed in Table 6:

**Part 3**

**Overview**

The scope of ISO 6336-3:2016, [6], is defined as follows:

“This document specifies the fundamental formulae for use in tooth bending stress calculations for involute external or internal spur and helical gears with a rim thickness  $s_R > 0,5$  ht for external gears and  $s_R > 1,75$  mn for internal gears. In service, internal gears can experience failure modes other than tooth bending fatigue, i.e. fractures starting at the root diameter and progressing radially outward. This document does not provide adequate safety against failure modes other than tooth bending fatigue. All load influences on the tooth root stress are included in so far as they are the result of loads transmitted by the gears and in so far as they can be evaluated quantitatively.

This document includes procedures based on testing and theoretical studies such as those of Hirt, Strasser and Brossmann. The results are in good agreement with other methods. The given formulae are valid for spur and helical gears with tooth profiles in accordance with the basic rack standardized in ISO 53. They can also be used for teeth conjugate to other basic racks if the virtual contact ratio  $\epsilon_{\alpha n}$  is less than 2,5.

The load capacity determined on the basis of permissible bending stress is

**Table 8 Range of validity and limitations**

Property	2006 edition, limits	2019 edition, limits
Lowest applicable number of load cycles	10e3 cycles	10e3 cycles

		Virtual contact ratio of the virtual spur gear, $\epsilon_{\alpha n}$												
		1	1.1	1.2	1.3	1.4	1.5	1.6	1.7	1.8	1.9	2	2.1	2.2
Overlap ratio, $\epsilon_{\beta}$	0	1.000	1.000	1.000	1.000	1.000	1.000	1.000	1.000	1.000	1.000	0.700	0.700	0.700
	0.1	1.000	0.995	0.992	0.988	0.986	0.983	0.981	0.979	0.978	0.976	0.707	0.705	0.704
	0.2	1.000	0.991	0.983	0.977	0.971	0.966	0.962	0.958	0.955	0.951	0.707	0.704	0.701
	0.3	1.000	0.986	0.975	0.965	0.956	0.949	0.942	0.936	0.931	0.926	0.707	0.702	0.697
	0.4	1.000	0.982	0.966	0.953	0.941	0.931	0.922	0.914	0.907	0.900	0.707	0.700	0.694
	0.5	1.000	0.977	0.957	0.941	0.926	0.913	0.901	0.891	0.882	0.874	0.707	0.699	0.691
	0.6	1.000	0.972	0.949	0.928	0.910	0.894	0.880	0.868	0.856	0.846	0.707	0.697	0.688
	0.7	1.000	0.968	0.940	0.916	0.894	0.876	0.859	0.844	0.830	0.818	0.707	0.695	0.684
	0.8	1.000	0.963	0.931	0.903	0.878	0.856	0.837	0.819	0.803	0.788	0.707	0.694	0.681
	0.9	1.000	0.958	0.922	0.890	0.862	0.837	0.814	0.793	0.775	0.757	0.707	0.692	0.678
	1	1.000	0.953	0.913	0.877	0.845	0.816	0.791	0.767	0.745	0.725	0.707	0.690	0.674
	1.1	1.000	0.953	0.913	0.877	0.845	0.816	0.791	0.767	0.745	0.725	0.707	0.690	0.674
	1.2	1.000	0.953	0.913	0.877	0.845	0.816	0.791	0.767	0.745	0.725	0.707	0.690	0.674
	1.3	1.000	0.953	0.913	0.877	0.845	0.816	0.791	0.767	0.745	0.725	0.707	0.690	0.674
	1.4	1.000	0.953	0.913	0.877	0.845	0.816	0.791	0.767	0.745	0.725	0.707	0.690	0.674
	1.5	1.000	0.953	0.913	0.877	0.845	0.816	0.791	0.767	0.745	0.725	0.707	0.690	0.674
	1.6	1.000	0.953	0.913	0.877	0.845	0.816	0.791	0.767	0.745	0.725	0.707	0.690	0.674
	1.7	1.000	0.953	0.913	0.877	0.845	0.816	0.791	0.767	0.745	0.725	0.707	0.690	0.674
	1.8	1.000	0.953	0.913	0.877	0.845	0.816	0.791	0.767	0.745	0.725	0.707	0.690	0.674
	1.9	1.000	0.953	0.913	0.877	0.845	0.816	0.791	0.767	0.745	0.725	0.707	0.690	0.674
	2	1.000	0.953	0.913	0.877	0.845	0.816	0.791	0.767	0.745	0.725	0.707	0.690	0.674
2.1	1.000	0.953	0.913	0.877	0.845	0.816	0.791	0.767	0.745	0.725	0.707	0.690	0.674	

**Figure 3 Load distribution factor as a function of the  $\epsilon_{\beta}$  and  $\epsilon_{\alpha n}$ .**

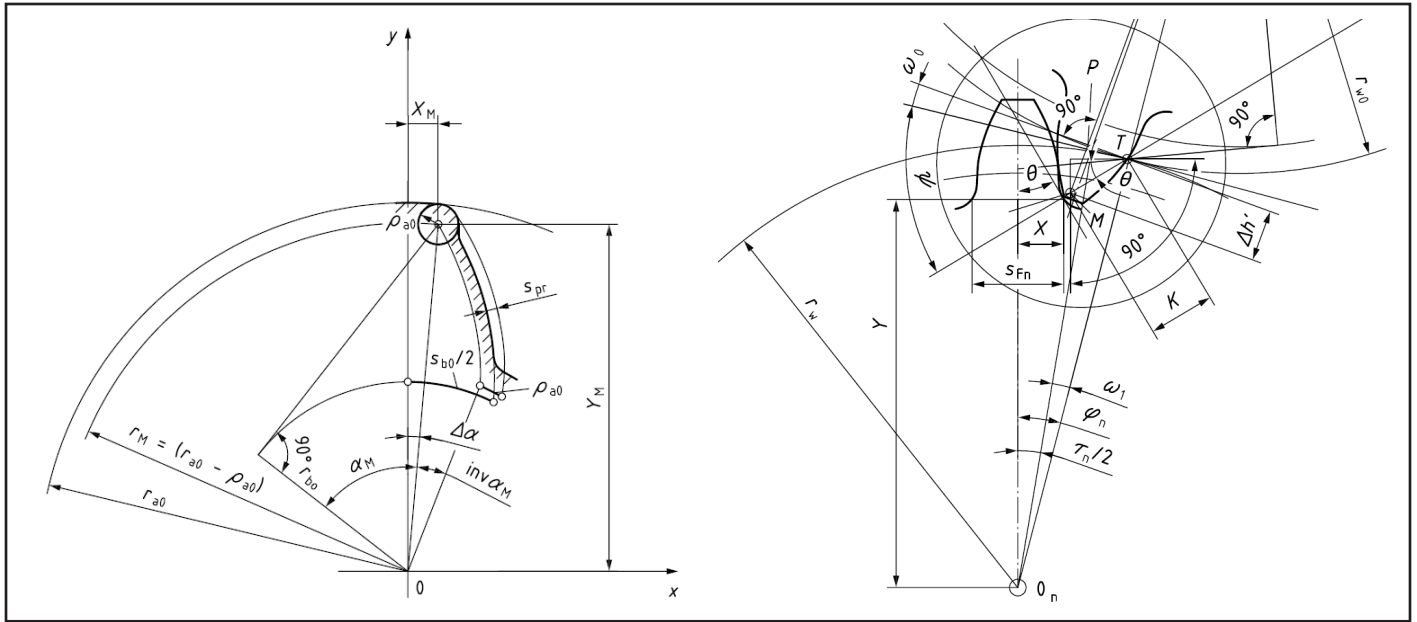


**Figure 4** Left: Quantities at the shaper cutter, (Ref. 6). Right: External gear in mesh with shaper cutter, coordinates  $X$  and  $Y$  of tangent point, tangent angle  $\theta$  and tooth thickness  $s_{Fn}$ , (Ref. 6). Tooth root fillet radius  $\rho_F$  and the bending moment arm  $h_{Fe}$  not shown explicitly.

termed “tooth bending strength.” The results are in good agreement with other methods for the range, as indicated in the scope of ISO 6336-1.”

### Structure of ISO 6336-3:2019, compared to previous edition

The structure of the foreword, introduction and sections 1 to 5 remain the same.

In section 6, the 2006 edition section 6.2.1 Tooth root normal chord,  $s_{Fn}$ , radius of root fillet,  $\rho_F$ , bending moment arm,  $h_{Fe}$  is replaced by sections 6.2.3 Tooth root normal chord,  $s_{Fn}$ , radius of root fillet,  $\rho_F$ , bending moment arm,  $h_{Fe}$  for external gears generated with a hob, 6.2.4 Tooth root normal chord,  $s_{Fn}$ , radius of root fillet,  $\rho_F$ , bending moment arm,  $h_{Fe}$  for external gears generated with a shaper cutter and 6.2.5 Tooth root normal chord,  $s_{Fn}$ , radius of root fillet,  $\rho_F$ , bending moment arm,  $h_{Fe}$  for internal gears generated with a shaper cutter.

Section 6.3 Derivations of determinant normal tooth load for spur gears has been moved to Annex C (informative) in 2019 edition.

The structure of sections 7 to 15 and Annex A (normative) again remain the same.

### Application

Further to the conditions for the application of ISO 6336 as found in part 1, see Table 2.

### Changes in formulas and factors

Load distribution influence factor  $f_{\epsilon}$  for the calculation of the form factor  $Y_F$  Compared to 2006 edition, in 2019 edition, the formula for the calculation of  $Y_F$  now contains a new factor  $f_{\epsilon}$ , the load distribution influence factor.  $Y_F$  as calculated in 2019 is equal to  $Y_F$  as calculated in 2006 edition, multiplied by  $f_{\epsilon}$ , both for external and internal gears. The factor  $f_{\epsilon}$  considers the influence of load distribution between the teeth in the mesh. It improves the results accuracy for gears with contact ratios  $\epsilon_{an} \geq 2.00$  (note that index  $n$  refers to the virtual spur gear). Contact ratios  $\epsilon_{an} \geq 2.00$  are reached for gears with high helix angles and or high transverse contact ratios  $\epsilon_{\alpha}$ . For gears with  $\epsilon_{an} < 2.00$ ,  $f_{\epsilon}$  becomes  $f_{\epsilon} = 1.00$  and the same values for  $Y_F$  result in 2019 edition compared to 2006 edition (except for the influence of the tooth thickness tolerance, see there). Note that the deep tooth factor  $Y_{DT}$ , for gears of high precision (ISO tolerance class  $\leq 4$ ) and  $2.00 \leq \epsilon_{an} \leq 2.50$  and with profile modifications to obtain a trapezoidal load distribution along the path of contact, does not change in 2019 edition compared to 2006 edition.

### Calculation of tooth root geometry for external gears generated with a shaper cutter

The calculation of tooth root geometry for external gears generated with a hob, section 6.2.3. in 2019 edition corresponds

to section 6.2.1 in 2006 edition (this section in 2006 edition is used for external gears generated with a hob or a shaper cutter and for internal gears generated with a virtual basic rack), with values and formulas “for external gears.”

For the calculation of tooth root geometry for external gears generated with a shaper cutter (and for internal gears, see below) however, a new section 6.2.4 (and 6.2.5 for internal gears, see below) with a new set of formulas is introduced in 2019 edition. These formulas originate from VDI 2737, Calculation of the load capacity of the tooth root in internal toothings with influence of the gear rim, 2016, (Ref. 16).

The formulas introduced in section 6.2.4 of 2019 edition are formulas No. (33) to (61) resulting in the coordinates  $X$  and  $Y$  of the tangent point (with tangent angle  $\theta = 30^\circ$  for external gears and  $\theta = 60^\circ$  for internal gears, see below), the tooth root thickness  $s_{Fn}$ , the tooth root fillet radius  $\rho_F$  and the bending moment arm  $h_{Fe}$ , as a function of the quantities at the shaper cutter.

### Calculation of tooth root geometry for internal gears

In 2006 edition, for internal gears, a virtual basic rack profile is used which differs from the basic rack profile in the tooth root radius  $\rho_{FP}$ . Formulas in section 6.2.1. “for internal gears” apply. In 2019 edition, for internal gears, only the shaper

cutter data is used. The calculation of the tooth root geometry (tooth root normal chord  $s_{Fn}$ , radius of root fillet  $\delta_F$  and bending moment arm  $h_{Fe}$ ) to derive form factor  $Y_F$  and stress correction factor  $Y_S$ , follows the same formula as used for external gears generated with a shaper cutter. However, negative signs are used for all diameters, and the manufacturing center distance  $a_0$  is used. Furthermore, the tangential angle  $\theta$  is  $\theta = 60^\circ$ .

### Influence of tooth thickness tolerances

In 2006 edition, form factor  $Y_F$  and stress correction factor  $Y_S$  are calculated from the nominal tooth form with the theoretical profile shift coefficient  $x$ . If the tooth thickness deviation near the root results in a thickness reduction of more than  $0.05 \times m_n$ , this shall be considered, by taking the generated profile,  $x_E$ , relative to rack shift amount  $m_n$  instead of the nominal profile. In 2019 edition, when the manufactured geometry is measured, it should be used. If not, then, based on the tooth thickness tolerance, the smallest generating profile shift,  $x_E$  min should be used to determine  $Y_F$  and  $Y_S$ .

### Helix angle factor $Y_\beta$

The tooth root stress of a virtual spur gear, calculated as a preliminary value, is converted by means of the helix factor,  $Y_\beta$ , to that of the corresponding helical gear. In 2019 edition, the formula to calculate  $Y_\beta$  has changed compared to 2006 edition, resulting in the values shown in Figure 5. Note that the value 1.00 is

Table 8 Range of validity and limitations		
Condition	2006 edition	2016 edition
Use with	ISO 6336-2, ISO 6336-3	ISO 6336-2, ISO 6336-3, ISO 6336-6
Use with	Application standards for industrial, high-speed and marine gears	Application standards for industrial, high-speed and marine gears
Applicable also	For rating of bevel gears along ISO 10300 series	For rating of bevel gears along ISO 10300 series
Limitations	Applicable to all gearing, basic rack profiles, profile dimensions, design, etc.	Applicable to all gearing, basic rack profiles, profile dimensions, design, etc.
Scope	Range indicated for scope of ISO 6336-1 and ISO 10300-1	Range indicated for scope of ISO 6336-1 and ISO 10300-1

substituted for  $\varepsilon_\beta$  when  $\varepsilon_\beta > 1.00$  and  $30^\circ$  is substituted for  $\beta$  when  $\beta > 30^\circ$ . Helix factors  $Y_\beta$  for  $\beta > 25^\circ$  shall be confirmed by experience.

### Relative notch sensitivity factor $Y_{\delta_{relT}}$ for static stress

The relative notch sensitivity factor  $Y_{\delta_{relT}}$  was defined in 2006 edition for normalized base steel (St), case-hardened wrought steel (Eh), flame or induction hardened wrought special steel (IF), nitrided wrought steel and nitriding steel (NT), through-hardened wrought steel, nitrided, nitrocarburized (NV), grey cast iron (GG) and modular cast iron (GGG). In 2019 edition, formulas to calculate the relative notch sensitivity factor for black malleable cast iron (GTS) are added in section 13.3.2.2, clause e).

### Part 5 Overview

The scope of ISO 6336-5:2016, (Ref. 8), is defined as follows:

“This document describes contact and tooth-root stresses and gives numerical values for both limit stress numbers. It specifies requirements for material

quality and heat treatment and comments on their influences on both limit stress numbers.” Furthermore, in the description of the scope of part 5, the application and limitation as listed in Table 8 are described.

### Structure of ISO 6336-5:2019, compared to previous edition

The structure of ISO 6336-5:2016, (Ref.8) is — with below exceptions — the same as in ISO 6336-5:2003, (Ref.7). Additional subsections have been introduced in 2016 edition:

- Section 4.4 on method Br for determination of allowable stress numbers.
- Annex A was normative in 2003 edition whereas it is informative in 2016 edition.

### Application

The conditions and limitations for application of ISO 6336-5 remain basically the same and are summarized in the table for the two editions, Table 8:

Minor changes in the normative references include:

- Some additional references are added (e.g., ISO 642, ISO 683-2, EN 10204 Metallic products — Types of inspection documents).

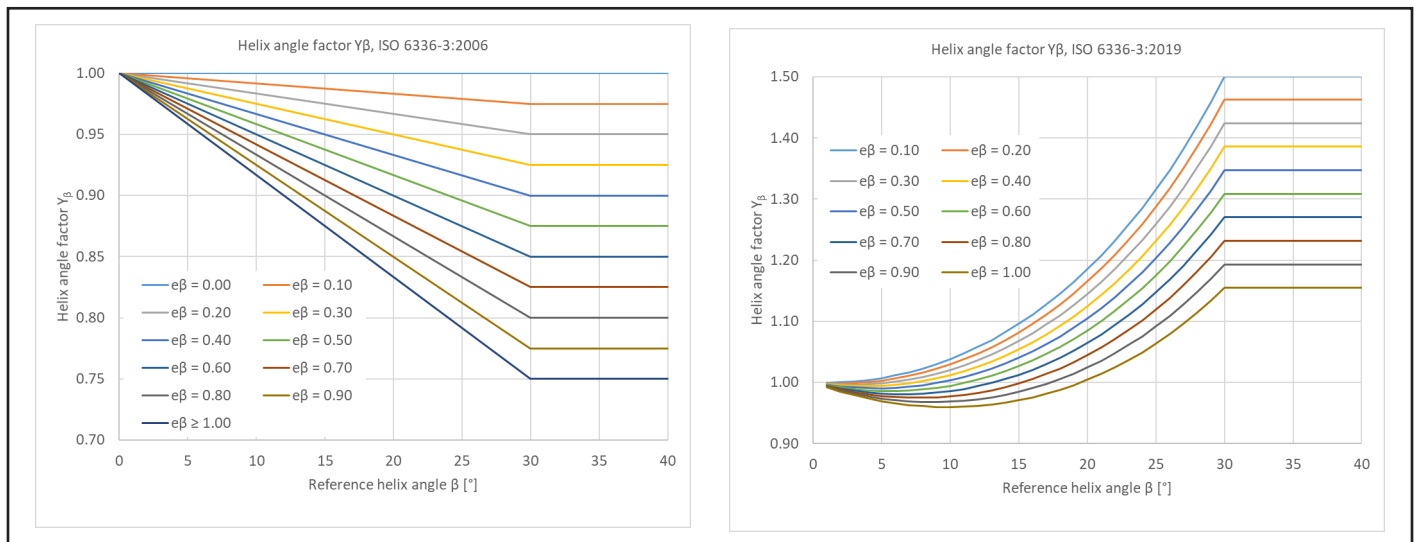


Figure 5 Helix angle factor  $Y_\beta$ . Left: along 2006 edition, Right: along 2019 edition.

- Year indicating revision of standards has been removed.
- Section 5.2 and 5.3.2: reference is made to ISO 1328-1. As ISO 1328-1 has been updated recently, the reference conditions are not necessarily the same anymore compared to ISO 6336-5: 2003.

### Changes in formulas and factors

In the new section 4.4, Method Br for methods for the determination of allowable stress numbers, the user is cautioned that "...contact stress numbers derived from rolling contact fatigue testing have to be used with caution since they tend to overestimate allowable contact stress numbers ..."

There are several minor changes and additions, but the permissible values typically used in gear rating are not changed. Changes include:

- Figure 5: Warning added for ME material grade for alloy steels "...relies heavily on the experience of the manufacturer..."
- Figure 14: Notes added with additional information on embrittlement due to white layer and aluminum containing nitriding steels.
- Figure 17+18, term "CHD" is used instead of "Eht" and "NHD" instead of "Nht".
- Figure 18: Maximum recommended NHD of 0.8mm is introduced. Values to determine hardness coefficient are moved to appendix B.2. A note is added regarding the use of heavier case depths for general designs.
- Table 3, item 3.1: some changes in the required cleanliness, conditions about calcium and oxygen content is moved to new items 3.2 and 3.3, item 4: requirements on grain size are now more specific, item 5.1: requirements on UT are now more specific, item 6: requirements for area reduction ratio now more specific, item 3: requirements on grain size are now more specific.
- Table 5, item 3: requirement that H2 content shall not exceed 2.5ppm, item 3.1: some changes in the required cleanliness, conditions about calcium and oxygen content is moved to new items 3.2 and 3.3, item 4: requirements for area reduction ratio now more specific, item 5: requirements on grain size are now more specific, item 10.4: permissible retained austenite level increased from 25% to 30%, magnetic particle inspection information removed.
- Table 8, item 7: "dwell time" removed, information on NHD added.
- Section 6.5: representative test bar size

changed.

- Section 6.7.1: standards for control of shot peening process added.
- Section 6.7.3; use of shot peening as a salvage operation, section added.

## Part 6

### Overview

The scope of ISO 6336-6:2016, (Ref. 10), is defined as follows:

"This document specifies the information and standardized conditions necessary for the calculation of the service life (or safety factors for a required life) of gears subject to variable loading for only pitting and tooth root bending strength."

It is noteworthy that this part 6 does not apply for other rating methods covered in ISO 6336 series, namely tooth flank fracture, scuffing and micropitting. Refer to the respective documents to find guideline on how to consider variable loads for these rating procedures.

### Structure of ISO 6336-6:2019, compared to previous edition

Section 4.1 and Annex B (informative) with guide values for the application factor  $K_A$  in ISO 6336-6:2006 has been removed in 2019 edition. They are now given in part 1, see Table 3 above. Otherwise, the structure of the document remains the same with edition 2019 as it was in edition 2006.

### Application

No specific information on application is given and those in parts 1, 2 and 3 apply.

### Changes in formulas and factors

In 2019 edition of this part 6, at the end of section 4.3 on the Palmgren-Miner rule, a sentence is added as follows: "... Other damage accumulation (including non-linear) hypotheses in addition to the herein described method and permissible damage sums other than one may be used upon agreement of the purchaser and the gear box manufacturer..." This now allows for the use of a permissible total damage different (typically smaller) than unity, or modified Miner's rule, e.g., using Haibach modification and total permissible damage  $D=0.50$  as shown in (Ref. 16) to match experiments.

Formulas and the calculation process in section 5 of edition 2019 have not changed compared to 2006 edition. However, the graphics have been extended and improved. For each step in the calculation process, a separate graphic is now available, explaining the calculation step by step.

An additional figure for the case where the life factor  $Z_{NT}$  or  $Y_{NT}$  is less than unity in the range of long life is also included as Figure 5 of the 2019 edition of this part, not shown here.

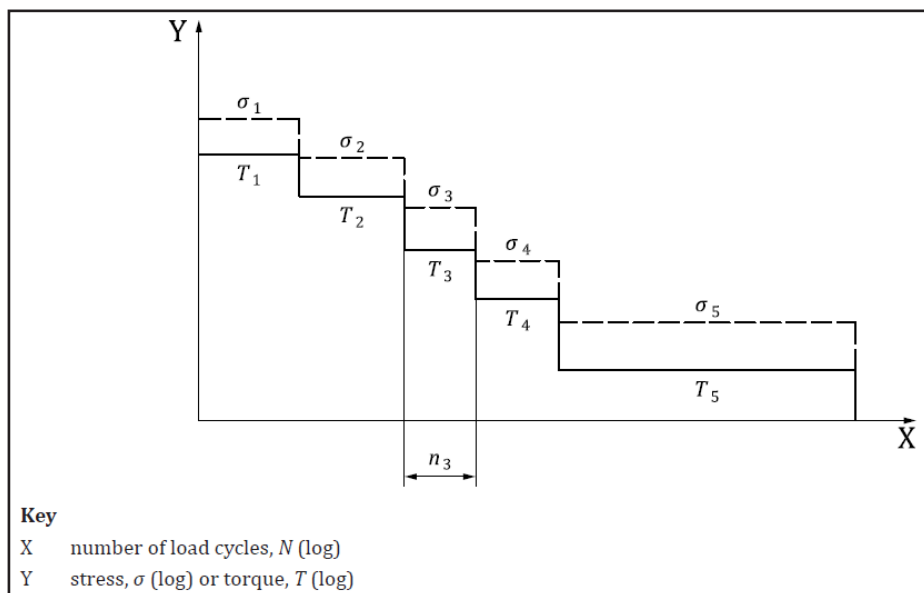


**Figure 6** Load and stress spectrum, Figure 2 in ISO 6336-6:2019. The figure explains how the load (torque) spectrum, represented by the torque levels  $T_i$ , associated with a speed level  $n_i$  each, is converted to a stress spectrum with stress levels  $\sigma_i$  (for speed levels  $n_i$ ), using the methods given in ISO 6336-2 and -3. Above and below figures were combined in one figure in 2006 edition, lacking some clarity.

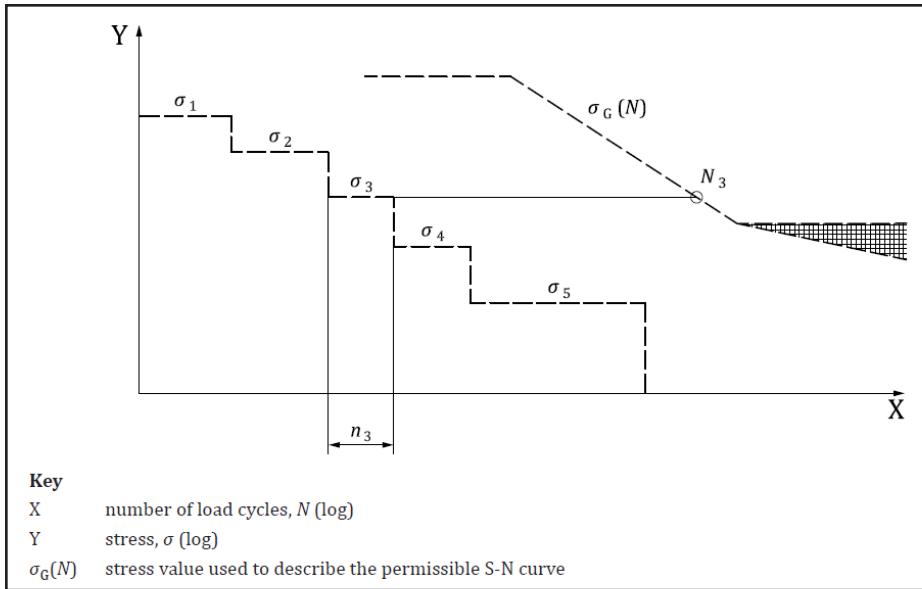


**Figure 7** Stress spectrum and S-N curve, Figure 3 in ISO 6336-6:2019. The figure explains how for a given stress level  $\sigma_i$ , an allowable number of load cycles  $N_i$  can be determined using the S-N curve(s) determined along ISO 6336-2 and -3. Note that the value  $\sigma_G$  is either  $\sigma_{HG}$  or  $\sigma_{FG}$ . Above two figures were combined in one figure in 2006 edition, lacking some clarity.

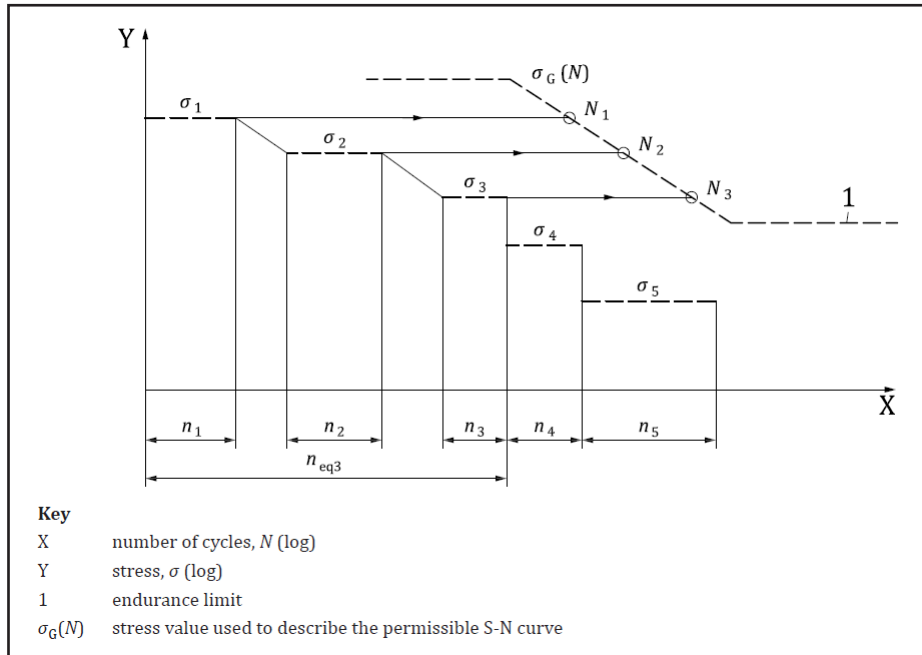


**Figure 8** Cumulated stress spectrum and fatigue curve limit when there is an endurance limit, Figure 4 in ISO 6336-6:2019. The figure explains how to represent the total accumulated damage  $U$  for the given load spectrum as the ratio  $n_{eqi}/N_i$  ( $i=3$  in this example) where  $\sigma_i$  is the lowest stress level still higher than the endurance limit. Note that the bins are shifted by drawing a line of the same slope than the S-N curve from the extremity of the stress bin  $\sigma_i$  to the stress level  $\sigma_{i+1}$ . This figure is new in edition 2016, adding clarity.

### Conclusion

The members of ISO TC 60/SC 2/WG 6 have contributed their expertise and time to advance ISO 6336. Industry experts and researchers have contributed new methods, run calculation examples with newly developed software and discussed how to improve the wording and structure of the document. The result is an even broader, more complex, practical and accurate tool aiming at increased gearbox power density, lowered risk of failures and deepened understanding of mechanisms governing the load capacity of cylindrical gears. Work does not stop here, under the guidance of the convenor, WG 6 is already working on the next edition of the documents.

The above changes will result in different load ratings, some of the differences are substantial, e.g., for internal gears or for helical gears without modifications. Users of ISO 6336 are advised to run extensive comparisons and gain experience using the third edition of ISO 6336. Further papers discussing the pros and cons of the changes or the implications on gear design are desirable. The influence of the changes on application standards and guidelines in specific industries is currently being discussed. This paper may help the engineers responsible for application standards and guidelines in adjusting e.g., K factors or required safety factors listed there.

While care has been taken to list all changes, the complexity of the document will have resulted in some changes having been overlooked. If so, readers' comments will be appreciated, thank you. 

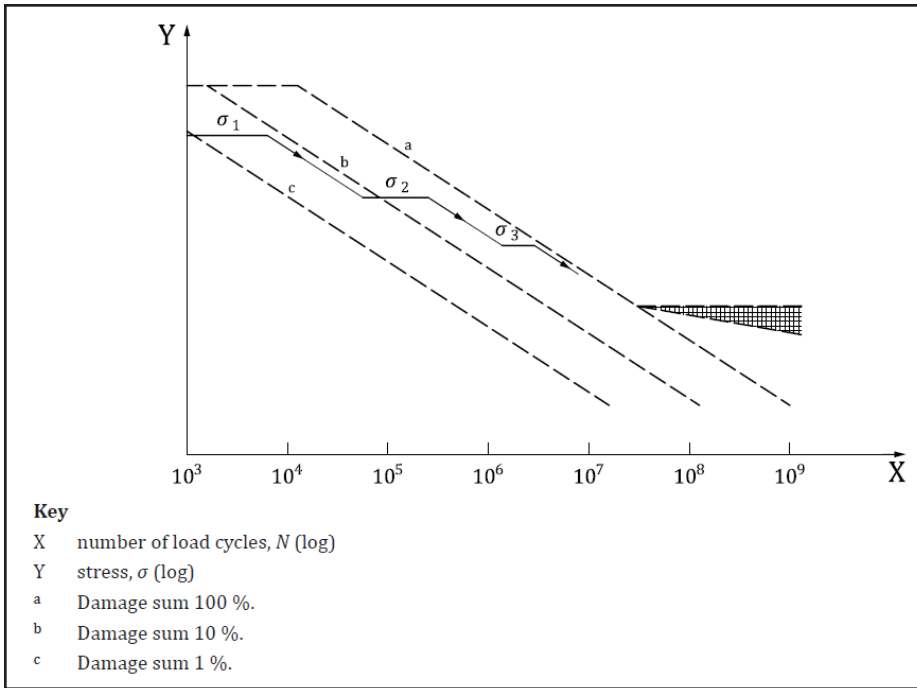


**Figure 9** Accumulation of damage, shown here for the first three bins (following bins are below endurance limit in this example). Accumulated damage  $U$  is  $U = n_{eq3} / N_3$ . Lines b and c are corresponding to line a (S-N curve determined along ISO 6336-2 or -3) but for higher probability of failure. This figure is the same in both editions.

## References

1. ISO 6336-1:2006, Calculation of load capacity of spur and helical gears – Part 1: Basic principles, introduction and general influence factors.
2. ISO 6336-1:2019, Calculation of load capacity of spur and helical gears – Part 1: Basic principles, introduction and general influence factors.
3. ISO 6336-2:2006, Calculation of load capacity of spur and helical gears – Part 2: Calculation of surface durability (pitting).
4. ISO 6336-2:2019, Calculation of load capacity of spur and helical gears – Part 2: Basic principles, introduction and general influence factors.
5. ISO 6336-3: 2006, Calculation of load capacity of spur and helical gears – Part 3: Calculation of tooth bending strength.
6. ISO 6336-3: 2019, Calculation of load capacity of spur and helical gears – Part 3: Calculation of tooth bending strength.
7. ISO 6336-4:2019, Calculation of load capacity of spur and helical gears – Part 3: Calculation of tooth flank fracture load capacity.
8. ISO 6336-5: 2003, Calculation of load capacity of spur and helical gears – Part 5: Strength and quality of materials.
9. ISO 6336-5: 2016, Calculation of load capacity of spur and helical gears – Part 5: Strength and quality of materials.
10. ISO 6336-6: 2006, Calculation of load capacity of spur and helical gears – Part 6: Calculation of service life under variable load.
11. ISO 6336-6: 2019, Calculation of load capacity of spur and helical gears – Part 6: Calculation of service life under variable load.
12. ISO/TR 6336-30:2017, Calculation of load capacity of spur and helical gears – Part 30: Calculation examples for the application of ISO 6336 parts 1,2,3,5.
13. ISO/TS 6336-22:2018(E) Calculation of load capacity of spur and helical gears – Part 22: Calculation of micropitting load capacity.
14. ISO 1122-1:1998, Vocabulary of gear terms – Part 1: Definitions related to geometry.
15. ISO 21771:2007, Gears — Cylindrical involute gears and gear pairs — Concepts and geometry.
16. ISO 53:1998, Cylindrical gears for general and heavy engineering – Standard basic rack tooth profile.
17. VDI 2737, Calculation of the load capacity of the tooth root in internal toothings with influence of the gear rim, 2016.
18. B.-R. Höhn, B.-R., P. Ostre, K. Michaelis, Th. Suchandt and K. Stahl. Bending Fatigue Investigation Under Variable Load Conditions on Case Carburized Gears, *AGMA FTM* 2000.
19. Kissling, U., J. Langhart, I. Tsikur and H. Dinner. ISO 6336:2019, Changes and implications, focus on root strength, [www.youtube.com/watch?v=zrNFAr57wCQ](https://www.youtube.com/watch?v=zrNFAr57wCQ) (8<sup>th</sup> April 2020).



**Hanspeter Dinner** studied mechanical engineering at the Swiss Federal Institute of Technology, Zürich, Switzerland and the National University of Singapore. He first worked as FEM engineer with a Swiss consultancy and as lead stress engineer with a roller coaster developer. He joined KISSsoft AG as software support and project engineer. In 2008, he started the consultancy company EES KISSsoft GmbH, representing the KISSsoft company in China, Japan, Korea, Taiwan and India. He has conducted about a hundred FEM, gear, bearings and transmission projects serving the wind, tractor, industrial gearbox and fine pitch gear industry. Since August 2019, he has been working in the function of Director Global Sales with KISSsoft – A Gleason Company.

